Partial Inhibition of Sarcoplasmic Reticulum Ca Release Evokes Long-Lasting Ca Release Events in Ventricular Myocytes: Role of Luminal Ca in Termination of Ca Release

Aleksey V. Zima, Eckard Picht, Donald M. Bers, and Lothar A. Blatter
Department of Physiology, Stritch School of Medicine, Loyola University Chicago, Maywood, Illinois

ABSTRACT In cardiac myocytes, local sarcoplasmic reticulum (SR) Ca depletion during Ca sparks is believed to play an important role in the termination of SR Ca release. We tested whether decreasing the rate of SR Ca depletion by partially inhibiting SR Ca release channels (ryanodine receptors) delays Ca spark termination. In permeabilized cat ventricular myocytes, 0.7 mM tetracaine caused almost complete Ca spark inhibition followed by a recovery significantly below control level. The recovery was associated with increased SR Ca load and increased Ca spark duration. Additionally, SR Ca release events lasting several hundred milliseconds occurred consistently. These events had a significantly lower initial Ca release flux followed by a stable plateau, indicating delayed release termination and maintained SR Ca load. Increasing SR Ca load (without inhibiting SR Ca release rate) or decreasing SR Ca release rate (without increasing SR Ca load) both induced only a small increase in spark duration. These results show that the combination of decreased release flux and increased SR Ca load has synergistic effects and exerts major changes on the termination of Ca release events. Long-lasting Ca release events may originate from highly interconnected release junctions where Ca diffusion from neighboring sites partially compensates Ca depletion, thereby delaying SR Ca-dependent termination. Eventually, these events terminate by luminal Ca-independent mechanisms, such as inactivation, adaptation, or stochastic attrition.

INTRODUCTION

Ca sparks are the elementary building blocks of the global sarcoplasmic reticulum (SR) Ca release during cardiac excitation-contraction coupling (1–3). During diastole, Ca sparks provide a major pathway for SR Ca leak, a process which has been implicated in reduced cardiac contractile force and arrhythmogenesis under pathological conditions such as heart failure (4). Sparks result from SR Ca release through a cluster of ryanodine receptors (RyRs) working as a functional unit. Irrespective of how Ca sparks are initiated (triggered or spontaneously), they occur as brief, spatially restricted elevations of cytosolic Ca. The short duration of Ca sparks suggests that potent mechanisms of SR Ca release termination exist despite the intrinsically self-regenerative nature of Ca-induced Ca release (CICR).

A model of local CICR (5) and experimental results (6–8) suggest that local SR Ca depletion is a major contributor to Ca spark termination and SR Ca release termination during a twitch. It has been proposed that Ca release during a spark reduces local SR [Ca] inducing RyR shutoff via a luminal Ca-dependent mechanism and does not necessarily lead to the exhaustion of the SR Ca store. According to lipid bilayer experiments, luminal Ca regulates RyR activity (9,10), presumably via Ca-dependent interaction of RyRs with the Ca binding protein calsequestrin (11). In isolated ventricular myocytes, SR Ca release is prolonged by increasing the functional amount of SR Ca, either by loading low affinity Ca buffers into the SR or by overexpressing calsequestrin (8,12). More direct evidence for the role of luminal Ca depletion in spark termination was obtained from simultaneous cytosolic and intra-SR free Ca measurements (13). This study revealed that Ca sparks lead to the depletion of free luminal Ca; however, replenishing of luminal Ca is significantly faster than refractoriness of local Ca release (or Ca spark restitution). These kinetic differences suggest that, in addition to local store depletion, other mechanisms, such as inactivation, adaptation, and stochastic attrition may also participate in Ca spark termination. If luminal Ca decline during a Ca spark is limited, then luminal Ca-independent mechanisms could become more important.

In this study, we tested the hypothesis that a slower depletion of luminal Ca by reducing SR Ca release flux delays termination and prolongs the duration of local Ca release events. We studied SR Ca release in isolated ventricular cardiomyocytes during partial inhibition of RyRs. These conditions induced Ca sparks with significantly longer duration, and two different populations of release events could be identified based on the duration distribution. Furthermore, release events with a stable plateau lasting several hundred milliseconds were readily observed. The maintained SR Ca release during the plateau may occur because local Ca replenishment by SERCA mediated uptake and diffusion from neighboring sites would prevent intra-SR Ca from declining to the threshold required for Ca-dependent release termination. Termination of long-lasting release events would then occur by Ca-independent mechanisms.

Submitted June 12, 2007, and accepted for publication October 31, 2007.

Address reprint requests to Aleksey V. Zima, 708-216-2054; E-mail: azima@lumc.edu.

Editor: Ian Parker.

0006-3495/08/03/1867/13 $2.00

doi: 10.1529/biophysj.107.114694

METHODS

Cell isolation

Cardiac ventricular myocytes were enzymatically isolated from adult cats using methods described previously (14). The procedure was approved by the Institutional Animal Care and Use Committee of Loyola University Chicago, Stritch School of Medicine.

Measurement and analysis of Ca sparks in permeabilized cat ventricular myocytes

Ca sparks were measured in permeabilized cardiomyocytes as described previously (15). The cell membrane was permeabilized by exposure to saponin (0.005% for 30 s). After permeabilization cells were placed in a solution composed of (mM): K aspartate 100; KCl 15; KH_2PO_4 5; MgATP 5; EGTA 0.35; $CaCl_2$ 0.12; $MgCl_2$ 0.75; phosphocreatine 10; HEPES 10; fluo-4 pentapotassium salt (Molecular Probes/Invitrogen, Carlsbad, CA) 0.03; creatine phosphokinase 5 U/ml; dextran (MW: 40,000) 8%, and pH 7.2 (KOH). Free [Ca] and [Mg] of this solution were 150 nM and 1 mM, respectively (calculated using WinMAXC 2.05, Stanford University, CA). All experiments were performed at room temperature. Changes in $[Ca]_i$ were measured with a laser scanning confocal microscope (Radiance 2000 MP, Bio-Rad, Hercules, CA) equipped with a 40× magnification oil-immersion objective lens (NA = 1.3). The Ca indicator fluo-4 was excited with the 488 nm line of an argon ion laser and fluorescence was measured at wavelengths >515 nm. Images were acquired in linescan mode (332 lines per second; pixel size 0.12 μm).

Ca sparks were detected and analyzed using SparkMaster (16) at a threshold criteria of 3.8. As shown before (16), this threshold criteria allows spark detection with a high sensitivity in combination with a very low frequency of false positive detections. However, when the analysis was performed with threshold criteria of 3.6 and 3.4, the results were qualitatively very similar (data not shown). Analysis included spark frequency (sparks $\times$ s^{-1} $\times$ $(100\ \mu m)^{-1}$), amplitude ($\Delta F/F_0$), full duration (ms), full width at half-maximal amplitude (μm), τ of decay (ms), maximal release flux (max($\Delta F/F_0$)/ms), and time-to-peak (ms). F_0 is the initial fluorescence recorded under steady-state conditions and $\Delta F = F–F_0$. The full duration (instead of the duration at half-maximal amplitude) was used to accurately quantify long-lasting Ca release events even when fluorescence during the plateau fell below the half-maximal amplitude.

SR Ca load was measured from the peak amplitude of the Ca transient induced by the rapid application of 20 mM caffeine for 3–4 s as used previously (8,15,17). This concentration of caffeine fully activates RyRs (18) and leads to the synchronized release of the total Ca stored in the SR. When SR Ca load was measured during partial inhibition of RyRs, caffeine was applied immediately after the removal of RyR inhibitors from the perfusion solution.

Measurement of Ca sparks in intact cat ventricular myocytes

Myocytes were loaded with fluo-4 by 20 min incubation in Tyrode's solution (in mM: NaCl 140; KCl 4; $CaCl_2$ 2; $MgCl_2$ 1; glucose 10; HEPES 10; pH 7.4) containing 20 μM fluo-4/AM (Molecular Probes/Invitrogen, Carlsbad, CA) at room temperature. Twenty minutes was allowed for deesterification of the dye. Because cat ventricular myocytes experience a gradual decrease in SR Ca load under resting conditions (rest decay), Ca sparks were measured under resting conditions after steady-state external field stimulation at a frequency of 1 Hz in the presence of 1 μM isoproterenol. Experiments were carried out at room temperature.

ADA loading

To increase SR Ca buffer capacity and therefore SR Ca load, permeabilized cells were incubated for 10 min with 5 mM of the low affinity Ca buffer *n*-(2-acetamido)iminodiacetic acid (ADA; $K_d \sim 0.2$ mM). Then, ADA was washed out and Ca sparks were studied in control solution. The slow diffusion of ADA out of the SR allows a time-frame of 10–15 min during which Ca sparks can be measured at high intraluminal SR Ca buffer capacity (8). Measurements of SR Ca load confirmed that stored Ca remained significantly higher for at least 10 min after ADA incubation.

Ryanodine receptor single channel recordings

SR vesicles isolated from cat ventricle were incorporated into planar lipid bilayers and RyR channel activity was measured as described previously (15). For recording of Cs currents through RyRs, the *cis*- and *trans*-chambers contained (mM): $CsCH_3SO_3$ 400 and HEPES 20; pH 7.3. The *cis*- and *trans*-chambers corresponded to the cytosolic and luminal side of the RyR channel, respectively. Free [Ca] in the *cis*-chamber was adjusted to 3 μM by adding an appropriate amount of EGTA, free [Ca] in the *trans*-chamber was adjusted to 100 μM. Single channel currents were recorded with an Axopatch 200B amplifier (Molecular Devices, Sunnyvale, CA) at a holding potential of −20 mV. Currents were filtered at 1 kHz and sampled at 5 kHz.

Drugs

All chemicals were purchased from Sigma-Aldrich (St. Louis, MO) unless otherwise stated. Phospholipids were obtained from Avanti (Alabaster, AL).

Statistics

Data are presented as mean ± SE of *n* measurements, except results of spark duration which are presented as mean ± SD. Statistical comparisons between groups were performed with the Student's *t*-test. The extra sum-of-squares F-test was used to test whether duration histograms are best fit with a single Gaussian distribution or the sum of two Gaussian distributions (analysis performed with GraphPad Prism 5.00). Differences were considered statistically significant at $p < 0.05$.

RESULTS

Partial RyR inhibition induces long-lasting SR Ca release events

We first established conditions at which RyR mediated SR Ca release flux was substantially but not completely inhibited. Representative examples of RyR single channel recordings in lipid bilayers under control conditions and in the presence of different RyR blockers are shown in Fig. 1 *A*. Tetracaine, 0.5 and 0.7 mM, instantaneously decreased RyR open probability (P_o) by 67 ± 8% ($n = 5$ bilayers) and 88 ± 5% ($n = 7$), respectively. Tetracaine concentrations >1 mM completely abolished RyR channel activity ($n = 4$). To avoid blocker-specific effects in the cellular experiments, we investigated ruthenium red and Mg as alternative RyR inhibitors. Ruthenium red (5 μM) or Mg (3 mM) exerted a comparable extent of RyR inhibition as 0.7 mM tetracaine (Fig. 1 *A*) and decreased P_o by 90 ± 6% ($n = 6$) and 85 ± 7% ($n = 5$), respectively. The single-channel amplitude and mean open time remained unchanged for the blockers tested here. Furthermore, none of the tested RyR inhibitors induced subconductance states.

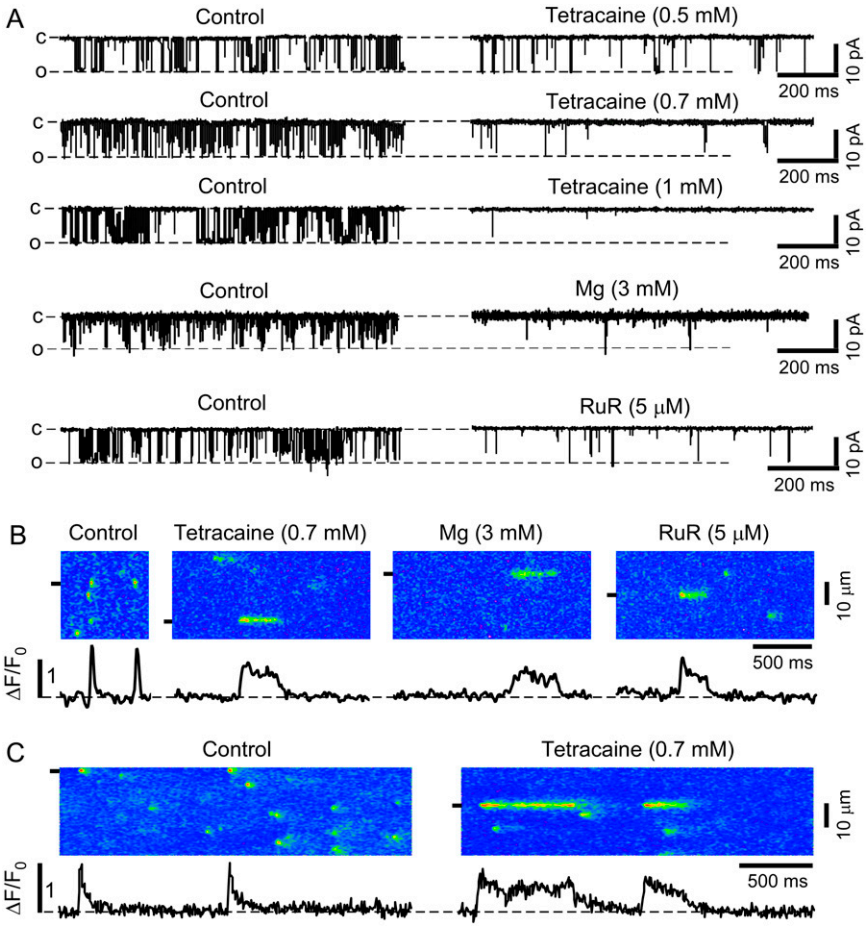

FIGURE 1 Effects of different RyR inhibitors on single RyR channel activity and elementary SR Ca release. (*A*) Representative RyR channel currents recorded under control conditions and after addition of tetracaine (0.5, 0.7, and 1 mM), Mg (3 mM), and ruthenium red (*RuR*; 5 μM) to the *cis*-side of the channel, respectively. All recordings were made at a holding potential of −20 mV and in the presence of 3 μM *cis*[Ca]. (*O*, open and *C*, closed channel level.) (*B*) Confocal linescan images and local $\Delta F/F_0$ profiles obtained from the regions marked by the black boxes under control conditions and after addition of tetracaine, Mg, and *RuR* in permeabilized ventricular myocytes. Recordings were made in different cells. (*C*) Ca sparks in intact ventricular myocytes under control conditions (*left*) and in the presence of 0.7 mM tetracaine (*right*). To induce stable spark activity, recordings were made in the presence of 1 μM isoproterenol.

When 0.7 mM tetracaine, 5 μM ruthenium red, or 3 mM Mg were applied to permeabilized myocytes, long-lasting Ca release events appeared consistently after initial inhibition of Ca sparks. Representative linescan images under control conditions and in the presence of tetracaine, ruthenium red, or Mg are shown in Fig. 1 *B*. We observed similar results with tetracaine in intact cardiomyocytes confirming that long-lasting SR Ca release events were not induced as an artifact of the membrane permeabilization (Fig. 1 *C*).

During partial inhibition of RyRs, prolonged Ca release events occurred in addition to typical sparks observed under control conditions. In the presence of tetracaine, Ca release sites showed a long-or-short behavior, where sites which showed long-lasting SR Ca release events did not show typical sparks under these conditions. Conversely, sites that showed typical sparks did not show long-lasting release events. Fig. 2 *A* illustrates this behavior in a 10-s long scan from the same position in a permeabilized myocyte: multiple long-lasting release events originated repeatedly from the same site. This site, however, did not show any typical sparks (fluorescence profile of this site shown below the linescan image). Typical short sparks originated from different release sites, which did not show prolonged-release events. Fig. 2 *B* shows the relationship between the duration of consecutive release events originating from the same release site. The duration of consecutive events showed a strong positive correlation ($R^2 = 0.7$), indicating that short release events are followed by other short events and that long release events are followed by other long-lasting events.

Reduced RyR activity increases SR Ca load

Partial inhibition of SR Ca release and uninhibited Ca uptake leads to increased SR Ca content (19–21). We therefore measured SR Ca load under our experimental conditions as the peak amplitude of Ca transients in response to rapid application of 20 mM caffeine. Representative linescan images and $\Delta F/F_0$ plots of caffeine-induced Ca transients are shown in Fig. 3 *A* for control conditions, 6 min after tetracaine application, and 3 min after tetracaine washout.

As expected for the equally effective concentrations of the RyR inhibitors used in these experiments, 0.7 mM tetracaine, 5 μM ruthenium red, and 3 mM Mg led to a comparable increase in SR Ca load (Fig. 3, *B–D*). After 6 min, SR Ca load increased to 177 ± 13% for tetracaine ($n = 16$ cells; $p < 0.05$), 182 ± 25% for Mg ($n = 6$ cells; $p < 0.05$), and 167 ± 16% for ruthenium red ($n = 5$ cells; $p < 0.05$).

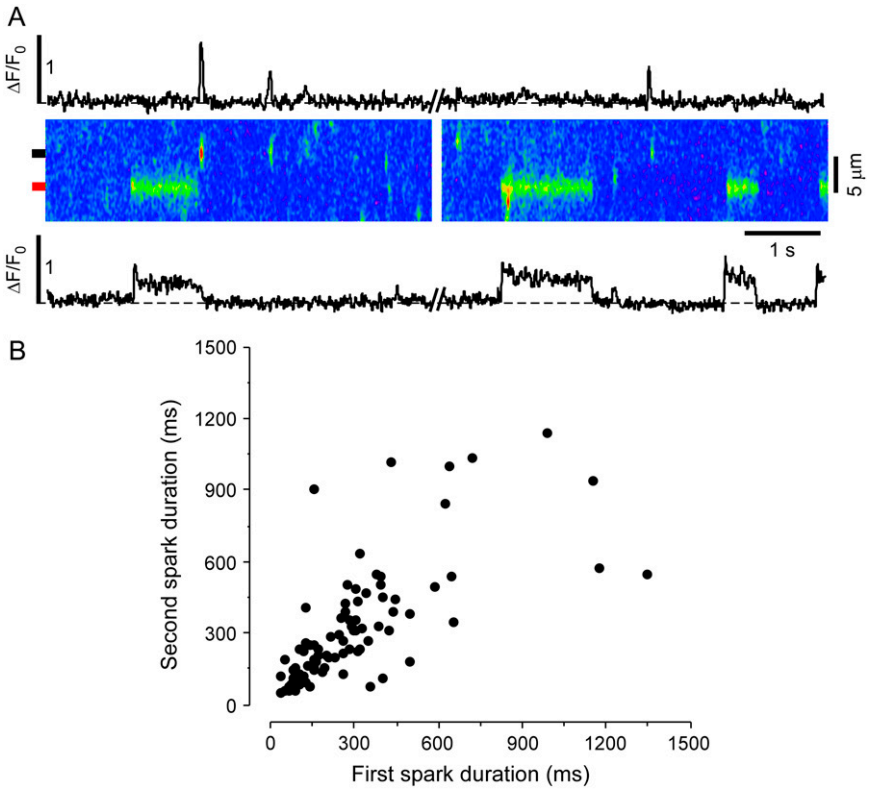

FIGURE 2 Long-or-short behavior of release sites in the presence of tetracaine. (*A*) 10 s linescan recording from the same position in a permeabilized myocyte. Release sites show either short or long-lasting release events but not both. (*Top*) Profile plot with short sparks from the region marked by the black box to the left of the image. (*Bottom*) Profile plot showing long-lasting release events from the region marked by the red box to the left of the image. (*B*) Duration of consecutive release events from the same SR release site ($R^2 = 0.7$; $n = 89$ events).

SR Ca load gradually decreased after RyR inhibition by tetracaine was relieved. Thirty seconds after tetracaine washout, SR Ca load was still increased to 160 ± 8% ($n = 5$ cells; $p > 0.05$). However, 3 min after washout of tetracaine or Mg, SR Ca load decreased to control levels but remained elevated after washout of ruthenium red. These data indicate that the partial RyR inhibition used here leads to a sustained increase in SR Ca load over the time period measured. The occurrence of prolonged elementary SR Ca release events is therefore associated with inhibited SR Ca release and increased SR Ca load.

In the subsequent experiments we choose tetracaine to partially inhibit Ca release, because the effects on RyRs are fully reversible (in contrast to ruthenium red) and because tetracaine does not change the ratio of free ATP/MgATP (in contrast to Mg).

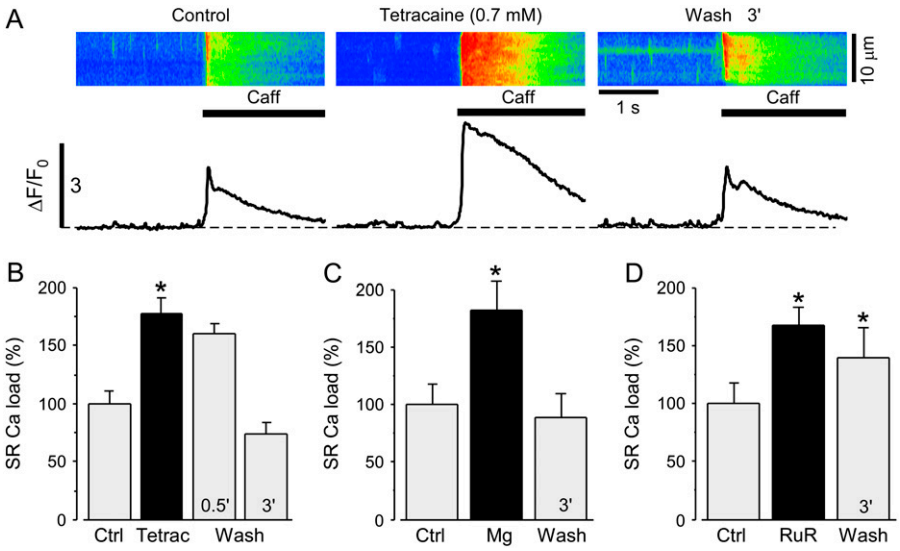

FIGURE 3 Effect of RyR inhibition on SR Ca load. (*A*) Confocal linescan images and corresponding $\Delta F/F_0$ profiles of Ca release induced by rapid application of 20 mM caffeine under control conditions, 6 min after addition of 0.7 mM tetracaine and 3 min after washout of tetracaine. Experiments were performed in permeabilized cardiomyocytes. $\Delta F/F_0$ profiles were obtained by averaging the entire cellular fluorescence from the linescan images. Average data of SR Ca load after application and washout of (*B*) tetracaine (0.7 mM), (*C*) Mg (3 mM), and (*D*) ruthenium red (*RuR*; 5 μM). Statistically different * at $p < 0.05$ versus control.

Tetracaine-mediated increase in SR Ca load induces a different population of elementary SR Ca release events

Next, we investigated in detail how partial inhibition of RyRs and the concomitant increase in SR Ca load affects elementary Ca release in permeabilized cardiomyocytes.

Fig. 4 *A* shows confocal linescan images and selected subcellular $\Delta F/F_0$ plots under control conditions, 0.5, 2, and 6 min after tetracaine application, and 0.5 and 3 min after tetracaine washout. Under control conditions, Ca sparks occurred at a frequency of 10.6 ± 0.8 sparks × s^{-1} × (100 μm)$^{-1}$ (n = 30 cells), and the duration histogram of the detected sparks could be well fitted with a Gaussian distribution (mean 47.5 ± 16 ms, Fig. 4 *B*, Control). Tetracaine caused initially almost complete inhibition of Ca sparks (spark frequency decreased to 0.8 ± 0.2 sparks × s^{-1} × (100 μm)$^{-1}$; $n = 30$; $p < 0.05$). Subsequently, spark activity gradually recovered (4.5 ± 0.4 sparks × s^{-1} × (100 μm)$^{-1}$; $n = 30$; $p < 0.05$) but did not reach the control level.

In the presence of tetracaine, the duration histogram progressively widened and developed a second peak that required a fit with the sum of two Gaussian functions (Fig. 4 *B*, Tetracaine). The total number of Ca release events during tetracaine application was separated into two populations based on the fit of the duration histogram. Both the mean ± SD of the duration and the number of events in each group

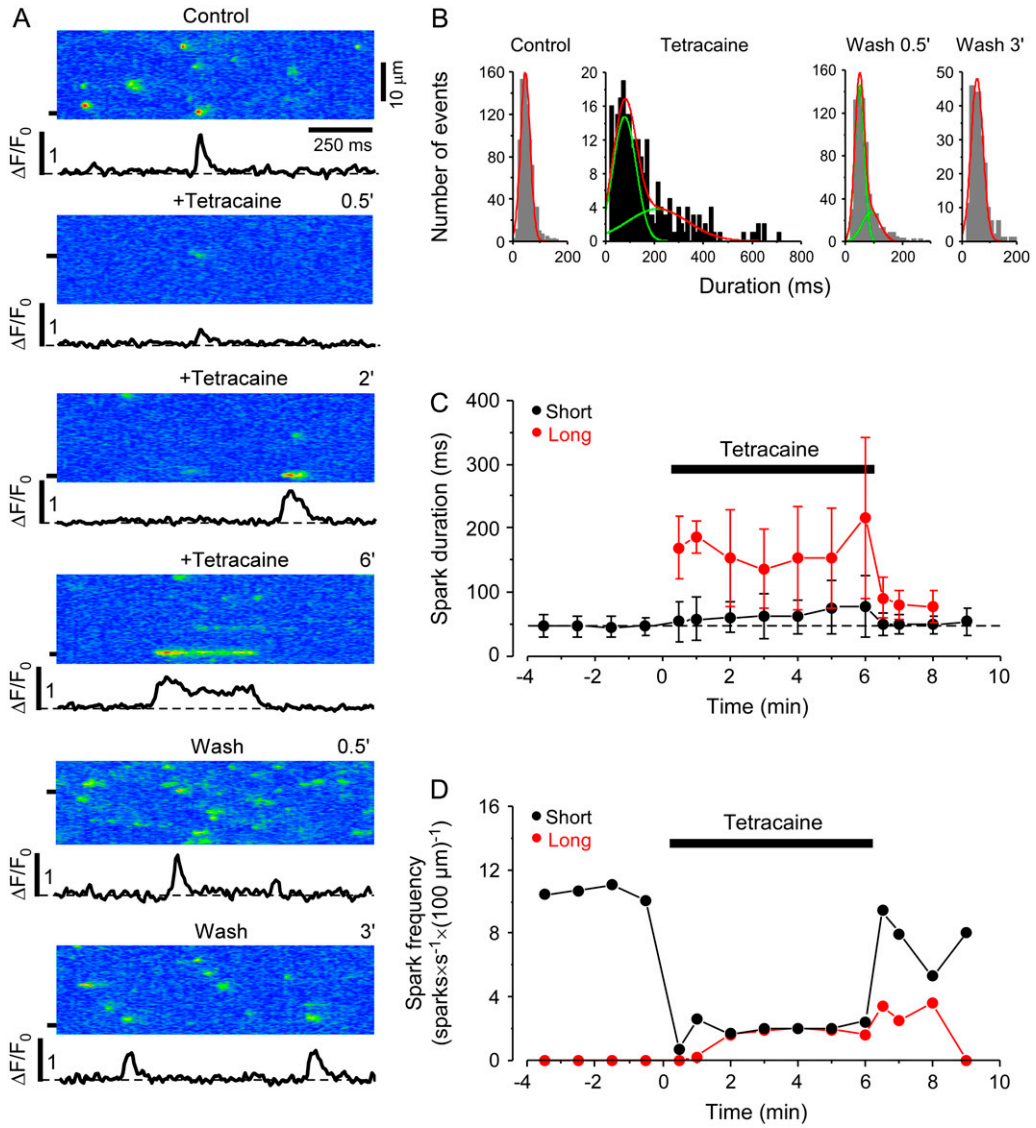

FIGURE 4 Effect of tetracaine on Ca spark frequency and duration. (*A*) Confocal linescan images of Ca sparks and corresponding local $\Delta F/F_0$ profiles under control conditions, 0.5, 2, and 6 min after addition of 0.7 mM tetracaine, and 0.5 and 3 min after washout of tetracaine. (*B*) Duration histograms of Ca sparks under control conditions, 6 min after tetracaine application, and after washout of tetracaine. (*C*) Full duration and (*D*) frequency of short and long Ca sparks under control conditions, during the application of 0.7 mM tetracaine, and after washout, respectively. Events were separated into two populations based on the fit of the duration histogram.

were calculated from the fit of the histograms. Fig. 4, *C* and *D*, show the effect of tetracaine on the full-duration and frequency of local release events separately for the two populations. The mean duration of the shorter events increased from 46 ± 14 ms, 30 s after tetracaine application, to 78 ± 48 ms after 6 min of tetracaine application ($p < 0.05$). The duration of the longer release events in the presence of tetracaine increased from 169 ± 49 ms, 30 s after tetracaine application, to 216 ± 125 ms after 6 min. In the presence of tetracaine, long and short events occurred at approximately the same frequency.

The effects of tetracaine were completely reversible after washout. After an initial increase of the spark frequency after washout (14.8 ± 1.3 sparks × s^{-1} × (100 μm)$^{-1}$; $n = 30$ cells; mainly due to an increase in the frequency of short events), spark frequency decreased to control levels (9.1 ± 0.9 sparks × s^{-1} × (100 μm)$^{-1}$) within 3 min. The duration histogram of the release events measured within 30 s after tetracaine washout was still best fit with the sum of two Gaussian distributions (Fig. 4 *B*, Wash 0.5′). The short peak had a mean duration similar to control conditions (49.8 ± 16.5 ms) and the second peak at 90.3 ± 31.5 ms was at a much shorter duration than the second peak in the presence of tetracaine. Also, the fraction of sparks in the long group after tetracaine washout was substantially smaller than with tetracaine (27% vs. 50%). Three minutes after the washout of tetracaine the duration histogram was comparable to control conditions with a single peak at 54 ± 22 ms (Fig. 4 *B*, Wash 3′).

In line with the results obtained in single channel experiments, higher concentrations of tetracaine (>1 mM) completely abolished spark activity without recovery during the presence of tetracaine. Even these high concentrations of tetracaine were completely reversible, indicating that no cell damage was induced during this protocol.

These results show that high SR Ca load and reduced release flux induce elementary Ca release events that are substantially longer than the typically observed Ca sparks under control conditions. Increased SR Ca load by itself, without the concurrent inhibition of SR Ca release, has similar effects as it also induces a second population in the duration histogram, but this effect was quantitatively much less pronounced. The following analysis describes these long-lasting release events in detail.

Characteristics of long-lasting Ca release events

Kinetic properties of elementary Ca release events provide important insights into Ca release, luminal Ca availability, and release termination. We therefore performed a detailed kinetic analysis of short sparks versus long-lasting Ca release events. As a threshold value for long-lasting events, we choose 3 × SD over the mean of the shorter peak (222 ms, calculated form the duration histogram in the presence of tetracaine shown in Fig. 4 *B*). This clearly separates long-lasting events from the population of shorter events and prevents mixing the two populations for the analysis. Fig. 5 *A* shows a representative image of a spark under control conditions and

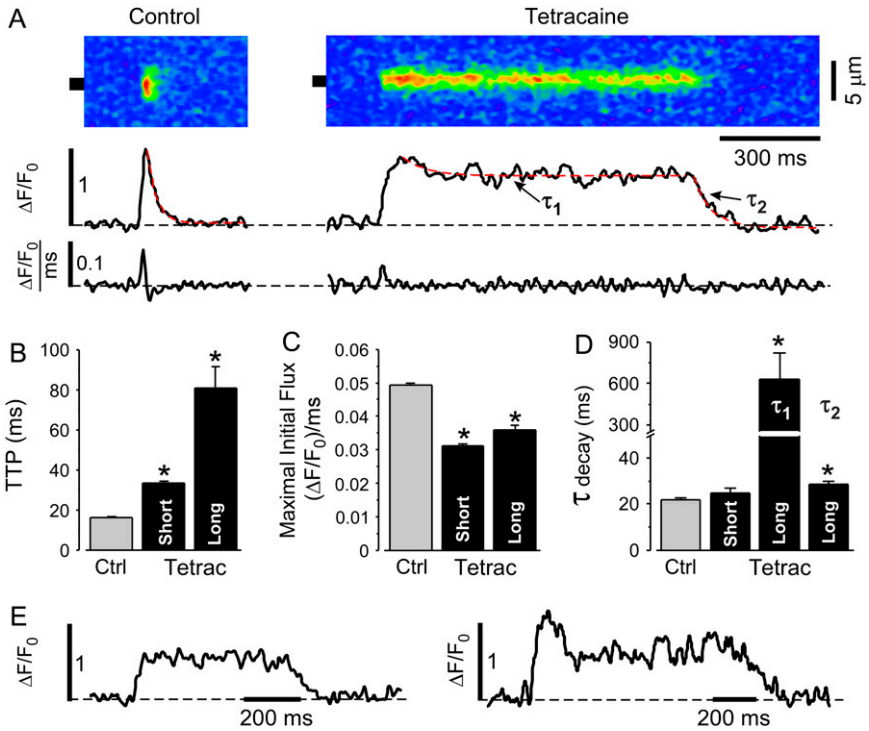

FIGURE 5 Effect of tetracaine on kinetic properties of elementary SR Ca release events. (*A*, *top*) Linescan images of a typical Ca spark under control conditions (*left*), and a long-lasting Ca release event in the presence of 0.7 mM tetracaine (*right*). Recordings were made in different cells. (*Middle*) Local $\Delta F/F_0$ profiles obtained by averaging the fluorescence from the regions marked by the black boxes. Dashed red lines show exponential fits of fluorescence decline during sparks. (*Bottom*) Ca release flux ($d(\Delta F/F_0)/dt$) derived from events shown on top. The scalebar shown under the linescan image applies to the images as well as to the graphs underneath the images. (*B*) Time-to-peak (*TTP*), (*C*) maximal initial Ca release flux, and (*D*) time constant of $[Ca]_i$ decline under control conditions, and in short and long release events after application of tetracaine. Two time constants describe the decay of long events in the presence of tetracaine: the initial decay to the stable plateau (τ_1) and for the final decay (τ_2). (*E*) Further examples of typical long-lasting Ca release events. Statistically different * at $p < 0.05$ versus control.

a long-lasting Ca release event that occurred after 4 min of tetracaine application. Fig. 5 *E* shows profile plots of other long-lasting Ca release events.

The peak Ca spark amplitude decreased from 0.66 ± 0.01 $\Delta F/F_0$ under control conditions ($n = 1918$ events) to 0.53 ± 0.01 $\Delta F/F_0$ in short sparks with tetracaine ($n = 802$ events) and to 0.58 ± 0.01 $\Delta F/F_0$ in long-lasting Ca release events in the presence of tetracaine ($n = 173$ events). Full width at half-maximal amplitude of Ca sparks decreased from 2.26 ± 0.02 μm under control conditions ($n = 1918$ events) to 1.93 ± 0.03 μm in short sparks ($n = 802$ events) but remained unchanged for long sparks (2.27 ± 0.06 μm; $n = 173$ events).

In comparison to sparks under control conditions and to short sparks in the presence of tetracaine, long-lasting Ca release events showed distinctively different kinetics. The time-to-peak provides an estimate of the duration of the initial Ca release flux (22). Long-lasting Ca release events had a substantially longer time-to-peak than sparks under control conditions or short sparks in the presence of tetracaine. On average, the time-to-peak increased from 16.3 ± 0.2 ms ($n = 1918$ events) under control conditions to 33.6 ± 0.9 ms ($p < 0.05$; $n = 802$ events) in short sparks with tetracaine and to 81.0 ± 10.6 ms ($p < 0.05$; $n = 173$ events) in long-lasting Ca release events in the presence of tetracaine (Fig. 5 *B*). These results indicate prolonged activity of RyR release clusters and delayed termination of initial Ca release in the presence of tetracaine, particularly with long-lasting release events.

The maximal SR Ca release flux (approximated from the first derivative of the cytosolic fluorescence (23,24)) was significantly reduced in short as well as in long events in the presence of tetracaine. Maximal Ca release flux was 0.049 ± 0.001 ($\Delta F/F_0$)/ms ($n = 1918$ events) in control and decreased to 0.031 ± 0.001 ($\Delta F/F_0$)/ms ($p < 0.05$; $n = 802$) and 0.036 ± 0.001 ($\Delta F/F_0$)/ms ($p < 0.05$; $n = 173$) in short and long events with tetracaine, respectively (Fig. 5 *C*). Although increased SR Ca load leads to an increased maximal release flux, the decreased flux under the conditions studied here indicates that the concomitant increase in SR Ca content does not compensate for the tetracaine effect of inhibiting release.

$[Ca]_i$ decay in normal sparks and in short sparks in the presence of tetracaine could be well described by single exponential time constants of 22.0 ± 1.0 ms and 24.8 ± 2.4 ms (difference is not significant; $n = 80$ events each), respectively. Long-lasting release events however, showed two decay phases: an initial slow decay after the peak fluorescence ($\tau_1 = 629 \pm 193$ ms, $n = 63$) and a second phase from the plateau of the first decay to basal fluorescence, which was similar to the decay of short sparks ($\tau_2 = 28.5 \pm 1.5$ ms; $n = 63$; Fig. 5 *D*).

The examples shown in Fig. 5 *E* illustrate the variation in the first decay phase ranging from a stable plateau after the initial increase in fluorescence (*left panel*) to a rapid decline after the peak to a level which can be below the half-max fluorescence (*right panel*). On average, the amplitude of the plateau was 65 ± 3% ($n = 63$ sparks) of the peak and remained relatively stable until termination occurred.

Decay kinetics of SR Ca release events are determined by cytosolic Ca diffusion and buffering, Ca uptake into the SR, and by maintained SR Ca release (25). As cytosolic Ca diffusion, buffering, and SERCA function are unaffected by tetracaine, differences in the decay kinetics between the different Ca release events described here can be attributed to maintained Ca release after the initial release.

In summary, the distinctly different kinetics of long-lasting SR Ca release events versus short sparks indicate that RyR clusters showing long-lasting release events are differently regulated when SR Ca load is high and release is inhibited. Possible mechanisms may include differences in local SR Ca load or local SR Ca refilling properties.

Relationship between long-lasting SR Ca release events, reduced release flux and increased SR Ca load

The following experiments were designed to test whether reduced SR Ca release flux or increased SR Ca load alone is sufficient to induce long-lasting SR Ca release events or whether both conditions must be present for these events to occur. Therefore, we performed experiments in which 1), SR Ca load was increased at uninhibited Ca release; and 2), Ca release was partially inhibited but SR Ca content was normal.

To increase SR Ca load, the low affinity Ca buffer ADA was loaded into the SR of permeabilized myocytes to increase the sarcoplasmic Ca buffer capacity (8). ADA incubation increased total SR Ca load to 136 ± 6% ($n = 7$ cells; $p < 0.05$) and subsequent application of tetracaine led to a further increase to 169 ± 9% ($n = 7$ cells; $p < 0.05$) and 191 ± 8% ($n = 7$ cells; $p < 0.05$) after 2 and 6 min, respectively (Fig. 6, *A* and *B*). Fig. 6 *C* shows typical linescan images obtained under control conditions, after ADA loading, and after tetracaine application and washout. After ADA incubation Ca spark frequency decreased from 11.5 ± 1.0 to 9.5 ± 0.8 sparks × s^{-1} × (100 μm)$^{-1}$ and the mean amplitude increased from 0.53 ± 0.01 $\Delta F/F_0$ at control to 0.62 ± 0.02 $\Delta F/F_0$ ($n = 16$ cells; $p < 0.05$).

Under control conditions, Ca sparks had a mean duration of 51.9 ± 20.8 ms and the duration histogram could be well fitted with a single Gaussian function (Fig. 6 *D*). After ADA loading, the duration histogram was best fitted with the sum of two Gaussian distributions (Fig. 6 *E*). However, the two duration distributions were relatively similar ($mean_{short} = 50 \pm 14$ ms; $mean_{long} = 78.5 \pm 28$ ms) in comparison to the alterations in Ca spark duration observed in the previous experiments where the longer population had a mean of 216 ± 125 ms 6 min after the application of tetracaine (Fig. 4 *B*). Based on the fit of the distributions 59% of the

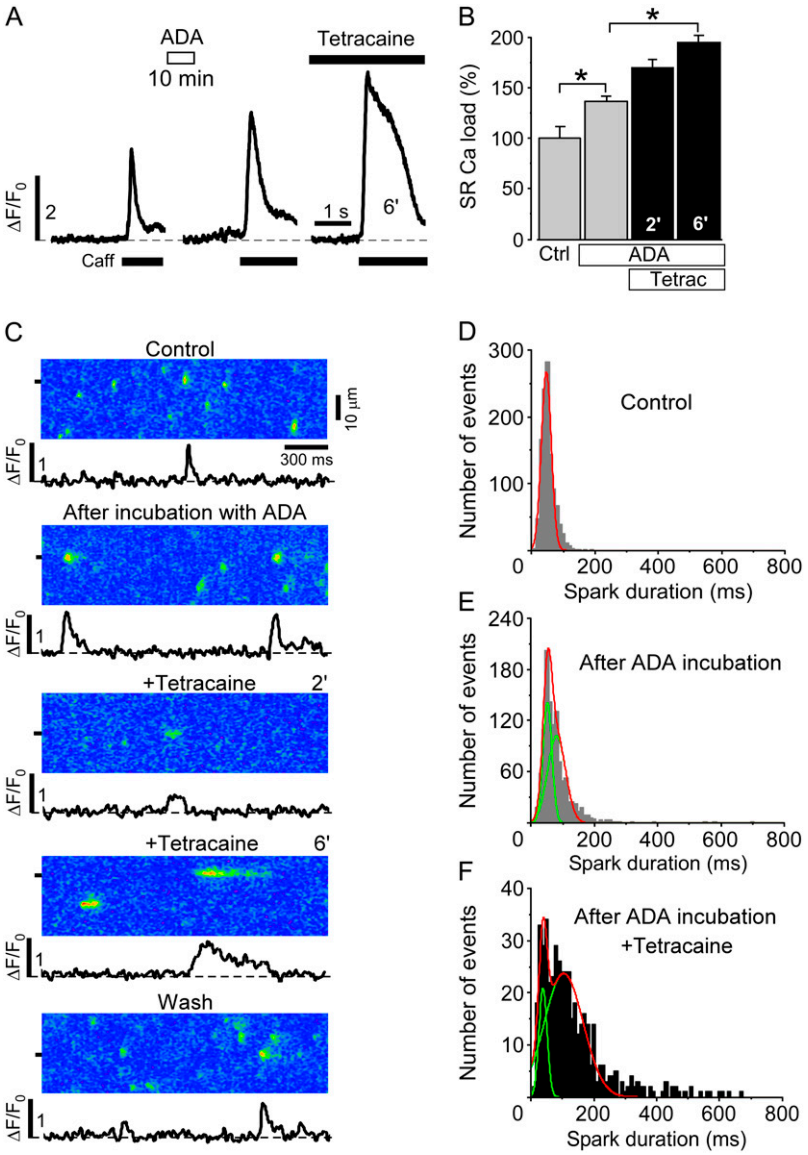

FIGURE 6 Effect of increased SR Ca buffering capacity on SR Ca release. (*A*) Caffeine-induced Ca release under control conditions, after 10 min incubation with ADA (5 mM) and 6 min after the subsequent addition of 0.7 mM tetracaine. (*B*) Normalized average data of SR Ca load after ADA incubation and after the subsequent application of tetracaine. (*C*) Linescan images of Ca sparks and corresponding local $\Delta F/F_0$ profiles under control conditions, after 10 min incubation with ADA, 2 and 6 min after addition of tetracaine (0.7 mM), and after washout of tetracaine. (*D*) Duration histograms of Ca sparks under control conditions, (*E*) after incubation with ADA, and (*F*) after the subsequent addition of tetracaine (averaged over 2 min from 4 to 6 min after tetracaine application). Statistically different * at $p < 0.05$ versus control.

events after ADA loading could be assigned to the longer distribution.

Prolonged release events lasting longer than 222 ms (the threshold used to distinguish long-lasting events from shorter events in the presence of tetracaine) occurred in ADA loaded myocytes only at a very low frequency but became much more numerous after the subsequent application of tetracaine, which also led to a further shift of the second population toward longer duration ($mean_{long} = 104 \pm 61$ ms, Fig. 6 *F*). Tetracaine application after ADA treatment resulted in even a larger fraction of release events being in the long duration group versus tetracaine alone (84% vs. 50%) (Fig. 4 *B* versus Fig. 6 *F*).

The results with ADA pretreatment are similar to the results obtained immediately after tetracaine washout (Fig. 4 *B*, Wash 0.5′) and show that high SR Ca load by itself is able to induce changes in the spark duration distribution and therefore modulates the release termination process; however, the influence on release termination is far less pronounced than when combined with reduced SR release flux.

Next, we tested whether inhibited SR Ca release alone is sufficient to induce prolonged Ca release events. The specific SERCA pump inhibitor thapsigargin was applied when long-lasting Ca release events were regularly observed after tetracaine application. Elementary release events were compared when SR Ca load had declined to control levels at inhibited SR Ca release.

Tetracaine increased SR Ca load to 176 ± 18% ($n = 7$ cells; $p < 0.05$) and subsequent application of thapsigargin (10 μM) gradually decreased SR Ca load to 77 ± 7% ($n = 7$ cells; $p < 0.05$) and 29 ± 9% ($n = 7$ cells; $p < 0.05$) after 3 and 7 min, respectively (Fig. 7, *A* and *B*). Fig. 7 *C* shows

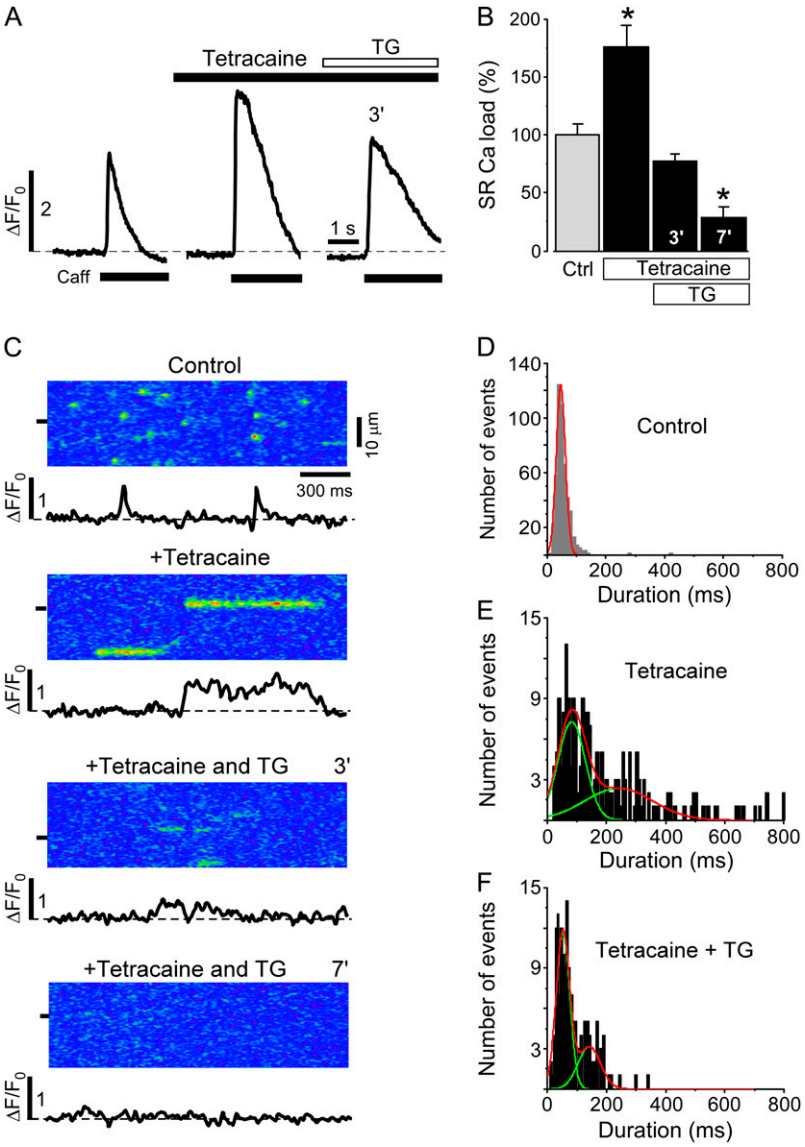

FIGURE 7 Effect of tetracaine on SR Ca load and Ca sparks during inhibition of SR Ca uptake by thapsigargin. (*A*) Caffeine-induced Ca release under control conditions, 3 min after the application of 0.7 mM tetracaine, and 3 min after the subsequent addition of 10 μM thapsigargin (*TG*). (*B*) Normalized average data of SR Ca load in the presence of tetracaine and after the subsequent application of thapsigargin. (*C*) Linescan images and corresponding local $\Delta F/F_0$ profiles under control conditions, 3 min after the application of 0.7 mM tetracaine, and 3 min and 7 min after the subsequent addition of 10 μM thapsigargin (*TG*). (*D*) Duration histograms of Ca sparks under control conditions, (*E*) after the application of 0.7 mM tetracaine (averaged from 2 to 3 min after tetracaine application), and (*F*) after the subsequent addition of thapsigargin (averaged over 2 min from 2 to 4 min after thapsigargin application). Statistically different * at $p < 0.05$ versus control.

representative linescan images and subcellular $\Delta F/F_0$ plots under control conditions, after tetracaine application, and 3 and 7 min after the subsequent addition of thapsigargin. As before, tetracaine application changed the duration histogram from a single Gaussian distribution under control conditions (46 ± 15 ms, Fig. 7 *D*) to a distribution that required a fit with the sum of two Gaussian distributions ($mean_{short}$ = 82 ± 46 ms; $mean_{long}$ = 242 ± 115 ms; Fig. 7 *E*).

After blocking SR Ca uptake with thapsigargin in the presence of tetracaine, the frequency of SR Ca release events gradually declined until no release events were observed. The duration histogram 3 min after thapsigargin application, when SR Ca load was close to control, still required a fit with two Gaussian functions (Fig. 7 *F*); however, the peak of the shorter duration at 53 ± 23 ms was very similar to the single peak of the histogram under control conditions. The second peak at 142 ± 38 ms contributed only to 31% of the total events and was at a much shorter duration than at the increased SR Ca load.

These data show that a reduction of the SR Ca release flux without changing the SR Ca content induces a prolongation of elementary SR Ca release events which becomes apparent by the second peak in the duration histogram. Conversely, high SR Ca load by itself induces similar changes in the spark duration distribution. However, when partial inhibition of SR Ca release is combined with increased SR Ca load, the effect on the spark duration distribution becomes much more pronounced.

DISCUSSION

Ca sparks result from the simultaneous opening of RyRs organized in clusters (release units) and occur as brief, spatially restricted elevations of cytosolic Ca (1–3,26). The short

duration of Ca sparks indicates that potent mechanisms exist that terminate SR Ca release despite the self-regenerative nature of CICR. Depletion of intra-SR free Ca ($[Ca]_{SR}$) during a Ca spark has been proposed as a key contributor to Ca release termination (for review, see (27)). Here, we tested the hypothesis that reduced SR Ca release flux delays Ca spark termination and prolongs elementary SR Ca release events. Any $[Ca]_{SR}$-dependent termination mechanism would then be less effective as $[Ca]_{SR}$ declines more slowly.

To decrease SR Ca release flux, we partially inhibited RyRs with tetracaine, Mg, or ruthenium red. This induced Ca sparks with significantly longer duration, and two different populations of release events could be identified based on the duration distribution. Furthermore, release events lasting several hundred milliseconds could be regularly observed in both intact and permeabilized myocytes (Fig. 1, *B* and *C*, and Fig. 4). When RyR inhibition was relieved, the duration distribution normalized and long-lasting release events disappeared entirely. The reversibility of the tetracaine-induced effects and the fact that these events could be completely abolished by depleting the SR with thapsigargin (Fig. 7) shows that these events are related to SR Ca release and did not arise as artifacts of membrane permeabilization or laser damage to the cells. In a previous study, the application of 5 μM ruthenium red did not evoke long-lasting Ca release events in permeabilized rat ventricular myocytes (17). It is likely that very subtle differences in the experimental conditions (e.g., the higher cytosolic Ca used in our experiments which leads to higher SR Ca load) might explain these differences.

A novel mechanism for long SR Ca release events?

Prolonged SR Ca release events have been previously described, after exposure to ryanodine, imperatoxin-A, FK506, or rapamycin, and were thought to be either the cellular correlate of long-lasting RyR subconductance states (2,28,29) or disrupted coupled gating allowing individual RyRs in a release cluster to independently open and close (5). Recently, Yang and Steele (30) reported perinuclear Ca release events in rat ventricular myocytes lasting for several seconds. However, the prolonged Ca release events described here appeared throughout the entire cytosol and were not associated with the perinuclear region.

The long-lasting SR Ca release events described here differ fundamentally from those described previously, because the RyR blockers used here do not disrupt coupled RyR gating (31), nor do they induce subconductance states or very long openings in lipid bilayers (Fig. 1 and (17,20,32)), even at high *trans*-[Ca] in bilayer studies (as expected in SR during RyR inhibition; data not shown, and (17,20,32)). Thus, how do long Ca sparks induced by ryanodine differ mechanistically from those described here with increased $[Ca]_{SR}$ and tetracaine? For ryanodine, single channel openings are prolonged up to 200 ms and may suffice to explain the long Ca sparks. In contrast, with tetracaine and increased $[Ca]_{SR}$, RyR single channel openings remain short (1–4 ms), therefore long channel open times may not explain the long release events. Rather, the long-lasting release events may result from continued RyR openings that are ''permitted'' because $[Ca]_{SR}$ fails to fall below a critical threshold that desensitizes the activation process. In a sense, this resembles typical repetitive RyR activity in lipid bilayers, where local Ca depletion on the luminal side is limited by the large volume of solution (so RyR openings can continue). This constitutes a novel paradigm, where the long release events here may be due to continuing single RyR activation, rather than delayed closure (as for ryanodine). In this sense, the macroscopic termination of local release here is not simply a scale-up of single channel, open time characteristics.

Decreased flux versus elevated SR Ca and long SR Ca release events

Low concentrations of tetracaine, Mg, or ruthenium red only transiently inhibit spark activity in cardiac myocytes (19–21,33). Under these conditions, increased SR Ca content and subsequent luminal Ca-dependent activation of RyRs overcomes the inhibitory effect. In contrast, the high concentration of tetracaine used here (0.7 mM), which decreases RyR P_o by ~90% in bilayer experiments (Fig. 1), induced a sustained decrease in Ca spark frequency (Fig. 4 *D*). This indicates that the autoregulatory capacity of the feedback between SR Ca load and stimulation of Ca release cannot compensate for this degree of RyR inhibition despite an almost doubled SR Ca content (Fig. 3). However, the increased SR Ca content in conjunction with the high degree of release inhibition regulates elementary SR Ca release in many aspects.

An isolated increase in SR Ca load or the sole reduction of SR Ca release flux both induced a slight prolongation of elementary SR Ca release events. When SR Ca load was increased by increasing the intra-SR Ca buffering capacity with exogenously added buffers (without altering SR Ca release, Fig. 6), Ca spark termination was only modestly delayed and individual Ca sparks became longer, similar to previous results (8). Although the duration histogram was best fitted with two Gaussian functions, the two populations had mean values which were very close. Likewise, Ca sparks immediately after the washout of tetracaine (when SR Ca content was comparable to the SR Ca load in the presence of tetracaine; Fig. 3 *B*) were only slightly prolonged and the duration distribution showed a small second peak very close to the dominating peak at a shorter duration (Fig. 4 *B*, Wash 0.5′). These findings are consistent with previous studies where increasing SR Ca load via phospholamban inhibitory antibody did not induce long-lasting SR Ca release events (33).

Additionally, reduction of SR release flux alone (at unaltered SR Ca content) induced a small Ca spark prolongation, but did not induce Ca release events lasting several hundred milliseconds (Fig. 7). Under these conditions, the duration histogram showed a small second population with a relatively short duration. These results show that the isolated increase in SR Ca load or the partial inhibition of SR release alone exert only minor effects on the termination of elementary SR Ca release events. However, the combination of these two perturbations has a synergistic effect and exerts major changes on the termination of Ca release events. When SR Ca release was partially inhibited and SR Ca load almost doubled, the duration histogram of these events showed a second population with a mean duration of 216 ± 125 ms. Even very long-lasting release events lasting several hundred milliseconds, and therefore far longer than typical for normal Ca sparks, occurred regularly under these conditions (Fig. 1, *B* and *C*; Fig. 2; and Figs. 4–7). We propose that the second population in the duration histogram is a direct result of altered termination and that long-lasting SR Ca release events exemplify this altered termination process at its extreme.

Long-lasting Ca release events had slightly smaller peak amplitudes followed by a plateau at 65% of the peak fluorescence. The initial maximal Ca release flux in the presence of tetracaine was only modestly reduced (by 37%) versus control and much higher than expected for the ~90% P_o reduction observed in bilayer experiments. Two factors could contribute to this: first, the increased SR-cytosolic Ca gradient leads to a higher flux through individual RyRs (34). Second, the tetracaine concentration required to achieve the same degree of RyR inhibition in permeabilized cells might be higher than in bilayer experiments. Thus, although the same concentrations were used for both types of experiments, the effective P_o reduction in the cellular setting may be lower than expected from bilayer experiments.

An interconnected SR network may limit local $[Ca]_{SR}$ depletion

The long plateau after the initial peak indicates maintained SR Ca release throughout the plateau phase. Furthermore, the fairly stable fluorescence during the plateau, without considerable decrease even over several hundred milliseconds (Fig. 5, *A* and *E*), suggests that intra-SR [Ca] remains relatively constant. Otherwise, the fluorescence would decrease as $[Ca]_{SR}$ depletes (5,28). Maintaining a constant $[Ca]_{SR}$ in the SR junction despite ongoing Ca release can potentially be explained by a highly interconnected intra-SR network as recently demonstrated by the direct measurement of intra-SR Ca (35,36). Intra-SR Ca diffusion from neighboring junctions could stabilize $[Ca]_{SR}$ during a release event and limit local $[Ca]_{SR}$ depletion.

Our finding that two different populations of SR Ca release events can be distinguished in the presence of tetracaine (and to a lesser extent by the isolated increase of $[Ca]_{SR}$ or decrease in release flux) suggests that some junctions are more extensively interconnected within the SR than other junctions. We propose that the Ca release events that comprise the long release event population originate from highly interconnected release sites and are therefore more depletion-resistant. The long-or-short behavior of release junctions in the presence of tetracaine (meaning that sites showing long-lasting events do not show short events (Fig. 2)) supports a structural (versus random) basis for the delayed termination of SR Ca release events under these conditions. Alternatively, local SR Ca load inhomogeneities as suggested by a study in a model of cardiac hypertrophy (37) might induce release events with different properties (e.g., based on local differences in SERCA/phospholamban expression or in RyR/phospholamban phosphorylation status). This seems unlikely, however, because even a less interconnected SR network as proposed based on electron-microscopic structural data (13) would equalize intra-SR [Ca] during diastole (36). Additionally, long-lasting release events have not been described after PKA or CaMKII stimulation of cardiomyocytes (38,39).

Final termination of Ca release by $[Ca]_{SR}$-independent factors

As $[Ca]_{SR}$ does not progressively deplete during the plateau of prolonged release events, the eventual termination of Ca release from highly interconnected junctions would then occur by mainly $[Ca]_{SR}$ independent mechanisms. Potential mechanisms include cytosolic Ca-dependent inactivation (40), use-dependent inactivation (41), or adaptation (42). Studies of RyR gating properties showed that these processes occur on a relatively slow timescale (over hundreds of milliseconds) and can therefore not explain the termination of typical Ca sparks. However, these mechanisms could become important for the termination of long-lasting release events. Another mechanism which may be relevant for long spark termination is stochastic closing of all RyR channels in a release cluster (stochastic attrition (43)). Because stochastic attrition is very sensitive to the number of RyRs available for activation, this mechanism may become especially important for Ca spark termination in the presence of RyRs inhibitors where a smaller than normal number of RyRs are active (as with tetracaine).

The apparent contradiction that inhibition of RyRs leads to prolongation of SR Ca release duration can be explained by channel activation by high luminal Ca in combination with a reduced SR Ca release flux. The maintained Ca release during the plateau of long-lasting release events suggests that local SR depletion does not reach a level where release is terminated by low luminal Ca. It seems likely that, during decreased Ca release flux, local $[Ca]_{SR}$ depletion can be effectively compensated by Ca diffusion from neighboring regions of the SR and Ca uptake by SERCA.

We thank Dr. Tim Domeier for critically reading the manuscript.

This work was supported by National Institutes of Health grants No. HL80101 (to L.A.B. and D.M.B.), No. HL62231 (to L.A.B.), No. HL30077 (to D.M.B.), and American Heart Association grant No. AHA0530309Z (to A.V.Z.).

REFERENCES

1. Cannell, M. B., H. Cheng, and W. J. Lederer. 1995. The control of calcium release in heart muscle. *Science*. 268:1045–1049.
2. Cheng, H., W. J. Lederer, and M. B. Cannell. 1993. Calcium sparks: elementary events underlying excitation-contraction coupling in heart muscle. *Science*. 262:740–744.
3. Lopez-Lopez, J. R., P. S. Shacklock, C. W. Balke, and W. G. Wier. 1995. Local calcium transients triggered by single L-type calcium channel currents in cardiac cells. *Science*. 268:1042–1045.
4. Kubalova, Z., D. Terentyev, S. Viatchenko-Karpinski, Y. Nishijima, I. Gyorke, R. Terentyeva, D. N. da Cunha, A. Sridhar, D. S. Feldman, R. L. Hamlin, C. A. Carnes, and S. Gyorke. 2005. Abnormal intrastore calcium signaling in chronic heart failure. *Proc. Natl. Acad. Sci. USA*. 102:14104–14109.
5. Sobie, E. A., K. W. Dilly, C. J. dos Santos, W. J. Lederer, and M. S. Jafri. 2002. Termination of cardiac Ca^{2+} sparks: an investigative mathematical model of calcium-induced calcium release. *Biophys. J.* 83: 59–78.
6. Bassani, J. W., W. Yuan, and D. M. Bers. 1995. Fractional SR Ca release is regulated by trigger Ca and SR Ca content in cardiac myocytes. *Am. J. Physiol.* 268:C1313–C1319.
7. DelPrincipe, F., M. Egger, and E. Niggli. 1999. Calcium signaling in cardiac muscle: refractoriness revealed by coherent activation. *Nat. Cell Biol.* 1:323–329.
8. Terentyev, D., S. Viatchenko-Karpinski, H. H. Valdivia, A. L. Escobar, and S. Gyorke. 2002. Luminal Ca^{2+} controls termination and refractory behavior of Ca^{2+}-induced Ca^{2+} release in cardiac myocytes. *Circ. Res.* 91:414–420.
9. Gyorke, I., and S. Gyorke. 1998. Regulation of the cardiac ryanodine receptor channel by luminal Ca^{2+} involves luminal Ca^{2+} sensing sites. *Biophys. J.* 75:2801–2810.
10. Sitsapesan, R., and A. J. Williams. 1994. Regulation of the gating of the sheep cardiac sarcoplasmic reticulum Ca^{2+}-release channel by luminal Ca^{2+}. *J. Membr. Biol.* 137:215–226.
11. Gyorke, I., N. Hester, L. R. Jones, and S. Gyorke. 2004. The role of calsequestrin, triadin, and junctin in conferring cardiac ryanodine receptor responsiveness to luminal calcium. *Biophys. J.* 86:2121–2128.
12. Terentyev, D., S. Viatchenko-Karpinski, I. Gyorke, P. Volpe, S. C. Williams, and S. Gyorke. 2003. Calsequestrin determines the functional size and stability of cardiac intracellular calcium stores: Mechanism for hereditary arrhythmia. *Proc. Natl. Acad. Sci. USA*. 100: 11759–11764.
13. Brochet, D. X., D. Yang, M. A. Di, W. J. Lederer, C. Franzini-Armstrong, and H. Cheng. 2005. Ca^{2+} blinks: rapid nanoscopic store calcium signaling. *Proc. Natl. Acad. Sci. USA*. 102:3099–3104.
14. Rubenstein, D. S., and S. L. Lipsius. 1995. Premature beats elicit a phase reversal of mechanoelectrical alternans in cat ventricular myocytes. A possible mechanism for reentrant arrhythmias. *Circulation*. 91:201–214.
15. Zima, A. V., J. Kockskamper, R. Mejia-Alvarez, and L. A. Blatter. 2003. Pyruvate modulates cardiac sarcoplasmic reticulum Ca^{2+} release in rats via mitochondria-dependent and -independent mechanisms. *J. Physiol.* 550:765–783.
16. Picht, E., A. V. Zima, L. A. Blatter, and D. M. Bers. 2007. SparkMaster: automated calcium spark analysis with ImageJ. *Am. J. Physiol. Cell Physiol.* 293:C1073–C1081.
17. Lukyanenko, V., I. Gyorke, S. Subramanian, A. Smirnov, T. F. Wiesner, and S. Gyorke. 2000. Inhibition of Ca^{2+} sparks by ruthenium red in permeabilized rat ventricular myocytes. *Biophys. J.* 79:1273–1284.
18. Rousseau, E., and G. Meissner. 1989. Single cardiac sarcoplasmic reticulum Ca^{2+}-release channel: activation by caffeine. *Am. J. Physiol.* 256:H328–H333.
19. Eisner, D. A., A. W. Trafford, M. E. Diaz, C. L. Overend, and S. C. O'Neill. 1998. The control of Ca release from the cardiac sarcoplasmic reticulum: regulation versus autoregulation. *Cardiovasc. Res.* 38:589–604.
20. Gyorke, S., V. Lukyanenko, and I. Gyorke. 1997. Dual effects of tetracaine on spontaneous calcium release in rat ventricular myocytes. *J. Physiol.* 500:297–309.
21. Overend, C. L., D. A. Eisner, and S. C. O'Neill. 1997. The effect of tetracaine on spontaneous Ca^{2+} release and sarcoplasmic reticulum calcium content in rat ventricular myocytes. *J. Physiol.* 502:471–479.
22. Pratusevich, V. R., and C. W. Balke. 1996. Factors shaping the confocal image of the calcium spark in cardiac muscle cells. *Biophys. J.* 71:2942–2957.
23. Sipido, K. R., and W. G. Wier. 1991. Flux of Ca^{2+} across the sarcoplasmic reticulum of guinea-pig cardiac cells during excitation-contraction coupling. *J. Physiol.* 435:605–630.
24. Song, L. S., J. S. Sham, M. D. Stern, E. G. Lakatta, and H. Cheng. 1998. Direct measurement of SR release flux by tracking ''Ca^{2+} spikes'' in rat cardiac myocytes. *J. Physiol.* 512:677–691.
25. Gomez, A. M., H. Cheng, W. J. Lederer, and D. M. Bers. 1996. Ca^{2+} diffusion and sarcoplasmic reticulum transport both contribute to $[Ca^{2+}]i$ decline during Ca^{2+} sparks in rat ventricular myocytes. *J. Physiol.* 496:575–581.
26. Blatter, L. A., J. Huser, and E. Rios. 1997. Sarcoplasmic reticulum Ca^{2+} release flux underlying Ca^{2+} sparks in cardiac muscle. *Proc. Natl. Acad. Sci. USA*. 94:4176–4181.
27. Stern, M. D., and H. Cheng. 2004. Putting out the fire: what terminates calcium-induced calcium release in cardiac muscle? *Cell Calcium*. 35:591–601.
28. Satoh, H., H. Katoh, P. Velez, M. Fill, and D. M. Bers. 1998. Bay K 8644 increases resting Ca^{2+} spark frequency in ferret ventricular myocytes independent of Ca influx: contrast with caffeine and ryanodine effects. *Circ. Res.* 83:1192–1204.
29. Xiao, R. P., H. H. Valdivia, K. Bogdanov, C. Valdivia, E. G. Lakatta, and H. Cheng. 1997. The immunophilin FK506-binding protein modulates Ca^{2+} release channel closure in rat heart. *J. Physiol.* 500:343–354.
30. Yang, Z., and D. S. Steele. 2005. Characteristics of prolonged Ca^{2+} release events associated with the nuclei in adult cardiac myocytes. *Circ. Res.* 96:82–90.
31. Marx, S. O., J. Gaburjakova, M. Gaburjakova, C. Henrikson, K. Ondrias, and A. R. Marks. 2001. Coupled gating between cardiac calcium release channels (ryanodine receptors). *Circ. Res.* 88:1151–1158.
32. Meissner, G. 1994. Ryanodine receptor/Ca^{2+} release channels and their regulation by endogenous effectors. *Annu. Rev. Physiol.* 56:485–508.
33. Lukyanenko, V., S. Viatchenko-Karpinski, A. Smirnov, T. F. Wiesner, and S. Gyorke. 2001. Dynamic regulation of sarcoplasmic reticulum Ca^{2+} content and release by luminal Ca^{2+}-sensitive leak in rat ventricular myocytes. *Biophys. J.* 81:785–798.
34. Mejia-Alvarez, R., C. Kettlun, E. Rios, M. Stern, and M. Fill. 1999. Unitary Ca^{2+} current through cardiac ryanodine receptor channels under quasi-physiological ionic conditions. *J. Gen. Physiol.* 113:177–186.
35. Duncan, A. M., E. Picht, and D. M. Bers. 2005. Dynamic Ca movement within cardiac sarcoplasmic reticulum. *Circulation*. 112:11–57. (Abstr.)
36. Wu, X., and D. M. Bers. 2006. Sarcoplasmic reticulum and nuclear envelope are one highly interconnected Ca^{2+} store throughout cardiac myocyte. *Circ. Res.* 99:283–291.
37. Song, L. S., Y. Pi, S. J. Kim, A. Yatani, S. Guatimosim, R. K. Kudej, Q. Zhang, H. Cheng, L. Hittinger, B. Ghaleb, D. E. Vatner, W. J. Lederer, and S. F. Vatner. 2005. Paradoxical cellular Ca^{2+} signaling in

severe but compensated canine left ventricular hypertrophy. *Circ. Res.* 97:457–464.

38. Guo, T., T. Zhang, R. Mestril, and D. M. Bers. 2006. Ca^{2+}/Calmodulin-dependent protein kinase II phosphorylation of ryanodine receptor does affect calcium sparks in mouse ventricular myocytes. *Circ. Res.* 99:398–406.
39. Li, Y., E. G. Kranias, G. A. Mignery, and D. M. Bers. 2002. Protein kinase A phosphorylation of the ryanodine receptor does not affect calcium sparks in mouse ventricular myocytes. *Circ. Res.* 90:309–316.
40. Fabiato, A. 1983. Calcium-induced release of calcium from the cardiac sarcoplasmic reticulum. *Am. J. Physiol.* 245:C1–14.
41. Sham, J. S., L. S. Song, Y. Chen, L. H. Deng, M. D. Stern, E. G. Lakatta, and H. Cheng. 1998. Termination of Ca^{2+} release by a local inactivation of ryanodine receptors in cardiac myocytes. *Proc. Natl. Acad. Sci. USA.* 95:15096–15101.
42. Gyorke, S., and M. Fill. 1993. Ryanodine receptor adaptation: control mechanism of Ca^{2+}-induced Ca^{2+} release in heart. *Science.* 260:807–809.
43. Stern, M. D. 1992. Theory of excitation-contraction coupling in cardiac muscle. *Biophys. J.* 63:497–517.